

A stochastic model of hydraulic variations within stream channels

Michael J. Stewardson and Thomas A. McMahon

Department of Civil and Environmental Engineering, Cooperative Research Centre for Catchment Hydrology
University of Melbourne, Parkville, Victoria, Australia

Received 13 October 2000; revised 9 July 2001; accepted 13 August 2001; published 29 January 2002.

[1] This paper presents a stochastic model of the joint depth and velocity probability distribution in stream channels. Model input is restricted to simple measures of channel geometry. Hydraulic distributions are quantified using two independent hydraulic variables, each a function of velocity and depth, and varying either longitudinally or laterally within a stream channel. The stochastic model provides a useful tool for exploring relations between fine-scale hydraulic variations and channel geometry. One application is modeling fine-scale hydraulic habitat conditions in stream channels. *INDEX TERMS*: 1824 Hydrology: Geomorphology (1625); 1845 Hydrology: Limnology; *KEYWORDS*: velocity distribution; depth distribution; channel geometry; habitat; stochastic hydraulics

1. Introduction

[2] The spatial distribution of velocity and depth is a fundamental characteristic of stream channels. It is directly related to a range of important flow properties and processes including shear stress distributions, energy coefficients, solute diffusion, and sediment transport. Hydraulic variation can also be a primary factor regulating the structure of stream channel communities [Allan, 1995], and stream habitat models often rely on velocity and depth distributions [e.g., Milhous *et al.*, 1989]. To date, most studies quantify the spatial distribution of velocity and depth using numerical models developed from two- and three-dimensional forms of the equations of motion. Very few studies have attempted to quantify hydraulic variations in the probability domain. In some cases the simplicity of a probabilistic description of hydraulic variations may provide some advantages over the more detailed spatially explicit descriptions currently in use.

[3] There has been some interest in the probability distribution of point velocity at a single cross section because of its influence on energy coefficients and the number of velocity measurements required for an accurate estimation of stream discharge. On the basis of theoretical considerations, Dingman [1989] suggests that the probability distribution of point velocity at a single cross section can be described by a power law distribution. He showed that the point velocity distribution at nine cross sections in New Hampshire conformed to this distribution. Using the entropy maximization principle, Chiu [1989] derived an exponential form for the point velocity distribution at a cross section.

[4] Increasing attention on management of stream habitats has led to interest in the probability distributions of hydraulic variables along stream reaches rather than a single cross section. Singh [1989] sampled velocity (at 0.4 times the depth above the bed) and depth in nine reaches in central Illinois. Probability distributions of depth within each stream reach were found to be approximately normal, and the standard deviation in depth and velocity generally increased with catchment area and reach mean velocity, respectively. Lamouroux *et al.* [1995] and Lamouroux [1998] examined the probability distribution of point velocity and depth throughout stream reaches in France and Germany. These studies indicated that both depth and velocity distributions changed with increasing

discharge from an exponential shape to a bimodal distribution that can be represented by the weighted sum of the exponential and normal probability density functions.

[5] To date, there have been few attempts to characterize probability distributions of velocity and depth in streams, and available methods are intended for very specific uses. This paper uses theoretical considerations and samples of velocity and depth from a wide range of stream types to quantify the joint probability distribution of depth and velocity for general application in studies of fluvial processes. Depth-averaged rather than point velocity is used to allow some consideration of the covariance of velocity and depth based on analysis of depth-velocity pairs. Depth and velocity do not vary randomly throughout a stream reach; rather, they exhibit spatial organization as expressed by the equations of motion. Generally, velocity increases with depth across a channel, and velocity decreases with depth along a channel. As a result, velocity and depth are not independent variables, and the univariate depth and velocity distributions are not sufficient to define their joint distribution. To overcome this problem, depth and velocity are transformed to provide two independent variables, one that varies across the channel but is invariant along the channel the other that is invariant across the channel but varies longitudinally. The univariate probability distribution of these two transformed variables provides a simple, efficient, and comprehensive approach to describing hydraulic variations in stream channels. This paper also describes a stochastic model that predicts the univariate distributions of these two independent variables from easily derived channel geometry characteristics.

2. Description of Data

[6] This study uses 149 reach surveys for streams in Australia, New Zealand, South Africa, and Europe (see Tables 1 and 2). Each reach survey provides a set of velocity-depth pairs that represent a sample of hydraulic conditions throughout the reach at the time of the survey (Figure 1). These surveys were mostly to provide input data for habitat modeling, and, although these data have been supplied by a variety of agencies, the survey methods used to collect the data are similar. Samples generally consist of velocity and depth measurements taken across several cross sections with velocity measured at 0.4 times the depth above the bed (0.4Z) or, in a few cases, at 0.2Z and 0.8Z. Depending on

Table 1. Number of Reach Surveys Used From Different Regions

Region	Reach Surveys
Australia	61
France	37
United Kingdom	22
Scandinavia	20
New Zealand	6
South Africa	3
Total	149

the number of velocities available, the depth-averaged velocity is estimated using

$$\bar{u} = u_{0.4Z}, \quad (1)$$

$$\bar{u} = \frac{u_{0.2Z} + u_{0.8Z}}{2}, \quad (2)$$

or

$$\bar{u} = \frac{u_{0.2Z} + 2u_{0.4Z} + u_{0.8Z}}{4}. \quad (3)$$

In many cases the location of measurement points across the channel is not random; rather it is to provide a good description of lateral variations in velocity and depth. As a result, fewer measurements are taken where conditions are relatively uniform. To account for this nonrandom sampling strategy, it is common practice to weight measurements, using the width of a segment of the cross section occupied by the measurement, when calculating reach statistics from the sample values [Bovee, 1994]. For this study, segment width is estimated as half the distance between adjacent measurement points. Discharge for the 149 surveys ranges from 0.01 m³/s to 100 m³/s, and sample size varies between 20 and 500 depth-velocity pairs. These surveys encompass a broad range of stream types in upland and lowland streams and reaches subject to a variety of human disturbances including flow regulation.

3. Methodology

3.1. Independent Hydraulic Variables

[7] The covariance of depth-averaged velocity (\bar{u}) and depth (Z) means that the bivariate probability density function is not equal to the product of the univariate probability density functions. If two new variables ψ_a and ψ_b could be identified, which are each functions of velocity and depth and are independent, then the joint \bar{u} - Z probability density function could be obtained using the Jacobian of the inverse transformation [Beaumont, 1980], i.e.,

$$f(\bar{u}, Z) = \frac{\partial(\psi_a, \psi_b)}{\partial(\bar{u}, Z)} f(\psi_a, \psi_b) = \frac{\partial(\psi_a, \psi_b)}{\partial(\bar{u}, Z)} f(\psi_a) f(\psi_b), \quad (4)$$

where the Jacobian is

$$\frac{\partial(\psi_a, \psi_b)}{\partial(\bar{u}, Z)} = \frac{\partial\psi_a}{\partial\bar{u}} \frac{\partial\psi_b}{\partial Z} - \frac{\partial\psi_b}{\partial\bar{u}} \frac{\partial\psi_a}{\partial Z}. \quad (5)$$

Using this approach, it would only require the univariate probability density functions $f(\psi_a)$ and $f(\psi_b)$ to characterize the joint \bar{u} - Z probability density function. If there was a transformation of velocity and depth, ψ_a that was invariant in the lateral

direction (across the channel) and another transformation and ψ_b that was invariant in the longitudinal direction (along the channel), these two transformed variables would be independent.

[8] Consider variations in velocity and depth across the cross section of a prismatic channel. An estimate of shear velocity is given by

$$u_* = \sqrt{gZs}, \quad (6)$$

and the depth-averaged velocity is given by

$$\bar{u} = \frac{u_*}{\kappa} \ln \frac{Z}{ez_0}, \quad (7)$$

where g is acceleration due to gravity, s is the friction gradient, z_0 is roughness height, and κ is the von Karman constant. These equations assume uniform two-dimensional flow conditions (i.e., neglecting velocity variations across the channel) and a logarithmic vertical velocity profile [French, 1986], assumptions that are violated in most natural streams. However, this approximation is considered adequate for the purpose of developing independent transformations of velocity and depth. Taking $a = \sqrt{gZs}/\kappa$ and substituting (6) into (7) gives

$$-a \ln z_0 = \frac{\bar{u}}{\sqrt{gZ}} - a \ln Z. \quad (8)$$

Assuming roughness height and the friction gradient are constant across a channel, the left-hand expression in (8) is invariant across the channel and provides an expression for ψ_a , i.e.,

$$\psi_a = \frac{\bar{u}}{\sqrt{gZ}} - a \ln Z. \quad (9)$$

If a is small, the transformation resembles a form of the Froude number. When considering the accuracy of assumptions regarding lateral variations in velocity, roughness height, and friction gradient, it is important to remember the purpose of this analysis is to derive two independent transformations of velocity and depth. The assumptions required to derive this transformation are examined in section 5 in light of tests of independence of ψ_a and ψ_b .

[9] To derive an expression for ψ_b , consider again the situation of two-dimensional flow. By the principle of continuity the unit discharge is constant along the channel and is therefore a suitable expression for ψ_b , i.e.,

$$\psi_b = \bar{u}Z. \quad (10)$$

The independence of the two hydraulic variables (ψ_a and ψ_b) is tested using the χ^2 test of independence, calculated using categorical data [Devore, 1987]. For this test each pair of ψ_a and ψ_b values for a particular reach survey are classified into one of 16 categories. A 4×4 table is used with categories for each variable defined by the ranges $[0, \psi_{0.25})$, $[\psi_{0.25}, \psi_{0.5})$, $[\psi_{0.5}, \psi_{0.75})$, and $[\psi_{0.75}, \infty)$, where $\psi_{0.25}$, $\psi_{0.5}$, and $\psi_{0.75}$ are the quartiles of ψ_a or ψ_b (based on counts rather than width-weighted samples). The χ^2 statistic is calculated using

$$\chi^2 = \sum_{i=1}^k \frac{(nb_i - np_i)^2}{np_i}, \quad (11)$$

where b_i is the proportion of the sum of weights (i.e., segment widths as explained above) for the i th sample, n is the number of \bar{u} - Z pairs that have been sampled for the particular reach survey, and p_i is the probability that an observation will be in the i th

Table 2. Reach Survey Data

Stream Name	Discharge, m ³ /s	Number of Z-u Pairs	Number of Cross Sections	Mean Width, m	Mean Hydraulic Depth	Mean Gradient, m/m	Country
Acheron	2.1	73	10	14.6	0.48	0.0024	Australia
Acheron	2.6	72	10	14.8	0.51	0.0024	Australia
Acheron	3.9	75	10	15.5	0.57	0.0024	Australia
alra ^a	4.65	284	9	26.3	0.9		France
ancela ^a	2.45	106	6	14	0.46		France
ancelb ^a	2.51	138	7	13	0.35		France
ance2 ^a	0.06	88	6	8.6	0.19		France
ance3a ^a	0.89	128	8	11.6	0.21		France
ance3b ^a	0.8	64	3	14.1	0.33		France
ance4 ^a	0.94	119	7	14.1	0.26		France
arc ^a	0.75	509	17	13.1	0.2		France
Armstrong	0.11	33	5	3.3	0.15		Australia
Armstrong	0.13	79	10	3.3	0.15	0.017	Australia
Armstrong	0.81	62	5	6.6	0.2		Australia
Armstrong	0.31	41	5	3.6	0.21		Australia
Armstrong	0.4	102	10	4.3	0.21	0.017	Australia
Armstrong	0.54	104	10	4.4	0.25	0.017	Australia
Armstrong	0.59	42	5	3.7	0.27		Australia
Armstrong	0.74	43	5	3.8	0.29		Australia
Armstrong	0.88	44	5	3.9	0.34		Australia
brav1 ^a	0.42	93	10	5.5	0.35		France
brav2 ^a	0.32	125	10	8.2	0.2		France
brav3 ^a	0.22	126	9	6.8	0.8		France
brevenne ^a	0.53	98	7	6.1	0.2		France
Broken	0.41	67	7	9.9	0.31	0.0019	Australia
Broken	0.39	135	7	9.9	0.35	0.0019	Australia
Broken	0.56	77	7	10.2	0.35	0.0019	Australia
Broken	2.1	174	7	13.1	0.54	0.0019	Australia
Broken	2.7	97	7	13.2	0.62	0.0019	Australia
cham1 ^a	0.07	106	8	5.1	0.19		France
cham2 ^a	0.11	118	9	5.7	0.24		France
cham3 ^a	0.17	116	8	7.6	0.27		France
Clutha	169	438	15	84.8	2.13	0.0012	New Zealand
Crystal	0.065	41	5	1.8	0.1		Australia
Crystal	0.049	47	5	2.1	0.11		Australia
Dalaa	4.25	208	11	22.6	0.33	0.00651	Norway
Dalaa	4.27	154	8	25.4	0.34	0.0007	Norway
Dalaa	10.23	212	7	49.8	0.38	0.00629	Norway
Dalaa	11.11	30	1	35.9	0.38		Norway
day ^a	0.13	159	10	6.2	0.2		France
dra ^a	2.12	50	5	9.6	0.37		France
Exe	0.12	98	10	3.4	0.21	0.0143	United Kingdom
Exe	0.21	105	10	3.3	0.26	0.0143	United Kingdom
Exe	0.86	119	10	3.8	0.38	0.0143	United Kingdom
Gowan	16.15	301	21	26.8	0.7	0.0029	New Zealand
Graceburn	0.036	63	12	3.3	0.09		Australia
Graceburn	0.14	67	8	4.5	0.11		Australia
Graceburn	0.17	70	8	4.7	0.14		Australia
Graceburn	0.18	69	12	4.6	0.14		Australia
Graceburn	0.22	69	8	4.5	0.14		Australia
Great Ouse	2.76	102	5	47.3	2.83	0.00092	United Kingdom
Great Ouse	5.92	100	5	47	2.92	0.00092	United Kingdom
guil1 ^a	2.53	246	11	20.9	0.27		France
Gwash	0.37	189	13	6.4	0.33	0.00058	United Kingdom
Gwash	1.16	101	7	7.6	0.38	0.00058	United Kingdom
Gwash	1.34	204	13	6.9	0.52	0.00058	United Kingdom
Hodder	2.22	120	8	20.7	0.24	0.00815	United Kingdom
Hodder	2.81	125	8	21.4	0.27	0.00815	United Kingdom
Hodder	5.25	133	8	22.8	0.34	0.00815	United Kingdom
Itchen	1.77	187	10	16	0.5	0.00084	United Kingdom
jab1 ^a	0.98	182	12	7.1	0.23		France
jab2 ^a	1.03	195	12	6.7	0.31		France
jab3 ^a	1.02	169	11	7.4	0.36		France
Juktan	3.71	79	3	20.1	0.25	0.00482	Norway
Juktan	2.75	49	2	16.6	0.31	0.0136	Norway
Juktan	3.28	161	6	19	0.31	0.0123	Norway
jul ^a	3.23	298	8	33.5	0.3		France
Lambourn	0.55	194	13	10.3	0.24	0.0017	United Kingdom
Lambourn	0.68	206	13	11	0.28	0.0017	United Kingdom
Lambourn	0.78	199	13	10.6	0.28	0.0017	United Kingdom
lig2 ^a	0.33	216	12	12.3	0.25		France
lig3 ^a	0.25	211	10	14.4	0.37		France

Table 2. (continued)

Stream Name	Discharge, m ³ /s	Number of Z-u Pairs	Number of Cross Sections	Mean Width, m	Mean Hydraulic Depth	Mean Gradient, m/m	Country
lig4 ^a	0.93	327	10	18.5	0.33		France
lig5 ^a	0.47	194	12	12.7	0.35		France
Lymington	0.092	164	12	7.2	0.23	0.00103	United Kingdom
Lymington	0.38	194	12	8.6	0.28	0.00103	United Kingdom
Lymington	0.59	199	12	8.9	0.3	0.00103	United Kingdom
Macquarie	0.73	101	7	13.9	0.46	0.0118	Australia
Macquarie	0.45	156	9	14.2	0.76	0.00201	Australia
Meander	4.37	272	14	20.3	0.64	0.00283	Australia
Meander	6.24	178	10	22.4	1.68	0.00025	Australia
Millstream	0.44	166	30	5.2	0.4	0.00163	United Kingdom
Moawhango	3.15	215	17	15	0.62	0.0016	New Zealand
oard1 ^a	6.59	302	12	32.6	0.63		France
oard2 ^a	7.05	303	11	27.4	0.51		France
Olifants	1.21	141	7	25.2	0.57	0.0028	South Africa
Olifants	3.18	165	7	35.2	0.7	0.0028	South Africa
Olifants	3.44	117	5	39.6	0.7	0.0022	South America
Patea	2.86	377	16	11.9	0.51	0.0093	New Zealand
Patersonia	0.027	129	10	5.3	0.06	0.00142	Australia
Patersonia	0.033	155	10	5.7	0.08	0.00142	Australia
Patersonia	0.053	113	10	5.5	0.08	0.00142	Australia
Patersonia	1.51	323	10	9.5	0.56	0.00142	Australia
pdv ^a	1.18	313	12	16	0.25		France
pin ^a	2.45	235	9	19.9	0.49		France
polon ^a	1.09	225	15	10.4	0.43		France
pra ^a	0.42	191	8	11.5	0.32		France
rho2 ^a	20.16	99	4	62.3	0.85		France
rho3 ^a	19.75	137	4	109	0.43		France
Ryans	0.035	143	12	6.2	0.13	0.006	Australia
Ryans	0.069	155	12	6.9	0.13	0.006	Australia
Ryans	0.16	172	12	7.6	0.15	0.006	Australia
Ryans	0.3	198	12	9.1	0.16	0.006	Australia
sap ^a	1.01	284	9	14.4	0.31		France
Seventime	0.045	106	10	3	0.16	0.0118	Australia
Seventime	0.48	141	10	4.1	0.26	0.0118	Australia
Silver	0.049	38	10	1.5	0.16		Australia
Silver	0.053	72	5	2	0.24		Australia
Silver	0.066	40	5	2.1	0.25		Australia
Silver	0.13	44	5	2.3	0.28		Australia
Silver	0.43	50	5	2.7	0.43		Australia
South Esk	9.08	205	12	23.7	0.91	0.00062	Australia
South Esk	6.01	155	8	31.7	1.09	0.002	Australia
Starvation	0.0079	102	10	2.2	0.1	0.017	Australia
Starvation	0.036	123	10	2.6	0.13	0.017	Australia
Starvation	0.072	28	5	3.2	0.14		Australia
Starvation	0.14	38	5	2.5	0.19		Australia
Starvation	0.46	40	5	4.4	0.22		Australia
Starvation	0.37	47	5	2.5	0.3		Australia
Starvation	0.53	47	5	2.5	0.36		Australia
Starvation	0.41	153	10	2.9	0.38	0.017	Australia
Starvation	0.71	45	5	2.5	0.41		Australia
Stjordalselva	13.44	64	2	44.3	0.45	0.00191	Norway
Suldalslagen	12.97	106	4	52.5	0.55	0.00249	Norway
Suldalslagen	15.27	60	3	39.3	0.64	0.00378	Norway
Suldalslagen	12.5	81	6	31.8	0.94	0.00099	Norway
Suldalslagen	47.47	93	3	59.5	0.97	0.00249	Norway
Suldalslagen	14.3	77	3	50.7	1.06	0.00233	Norway
Suldalslagen	13.76	148	6	48.5	1.09	0.00186	Norway
Suldalslagen	15.48	74	3	48.3	1.12	0.00241	Norway
Suldalslagen	47.04	75	3	46.4	1.12	0.00378	Norway
Suldalslagen	46.87	79	3	82.6	1.17	0.00186	Norway
Suldalslagen	50.6	50	2	48.6	1.31	0.00099	Norway
Suldalslagen	51.36	110	3	69.5	1.35	0.00241	Norway
Suldalslagen	49.31	88	3	55.9	1.49	0.00233	Norway
Tarago	0.4	66	5	6.5	0.22		Australia
Tarago	0.49	66	5	6.4	0.25		Australia
Tarago	0.45	58	5	5.7	0.38		Australia
Trout	0.14	138	10	3.9	0.12	0.0108	Australia
Trout	0.12	154	10	4.4	0.13	0.0108	Australia
Trout	0.62	193	10	5.6	0.24	0.0108	Australia
Waiari	4.12	302	18	9.3	0.99	0.0017	New Zealand
Waiwakaiho	2.39	436	17	15.8	0.41	0.0158	New Zealand
Watts	0.14	147	17	5.6	0.33		Australia

Table 2. (continued)

Stream Name	Discharge, m ³ /s	Number of Z-u Pairs	Number of Cross Sections	Mean Width, m	Mean Hydraulic Depth	Mean Gradient, m/m	Country
Wye	0.54	133	12	12.7	0.31	0.00557	United Kingdom
Wye	1.86	120	10	14.4	0.36	0.00557	United Kingdom
Wye	2.61	146	12	14.2	0.47	0.00557	United Kingdom
yon3 ^a	1.99	96	10	8.3	0.49		France
yon4 ^a	3.38	56	6	16.2	0.34		France

^a Codes are those used by *Lamouroux et al.* [1995].

category if the two transformed variables are independent. If the two transformations are independent, the χ^2 statistic for the 149 reaches should be distributed according to the χ^2 function with 9 degrees of freedom.

[10] For this study, a will be treated as a calibrated value and adjusted for each reach survey to provide a minimum value of χ^2 for the velocity-depth pairs provided by the survey rather than calculated using $a = \sqrt{s}/\kappa$. An attempt was made to use the calculated value, but substantially better results were achieved by calibration. It should be remembered that the intent of this analysis is to identify two independent transformations of depth and velocity, and the use of calibration is considered acceptable for this purpose. A macro written for Microsoft Excel[®] is used to select the value of a that minimizes χ^2 . Where stream gradient is known, the calibrated value of a is compared with the value calculated using $a = \sqrt{s}/\kappa$ (assuming $\kappa = 0.4$).

3.2. Stochastic Model

[11] This section provides the development of a stochastic model of the univariate distributions of ψ_a and ψ_b within a stream reach using data for the 149 field surveys. The stochastic model predicts parameters for a probability density function that approximates the distributions of the two independent variables. Input variables for the model are selected so that they can be derived from simple field measurements and one-dimensional hydraulic modeling.

[12] Both positive and negative values of ψ_a are possible where negative values are associated with low velocities in deeper sections of the stream. Since ψ_a is approximately constant across a channel, one might hypothesize that ψ_a has a centered probability distribution with a spread reflecting longitudinal channel variability. The value of ψ_a at shallow, fast flowing sections will be large, and in slow deep sections, ψ_a will be relatively small. For a channel with little longitudinal variation in channel geometry, ψ_a is likely to have a narrow distribution, and for a stream with greater variation in cross-section size and shape the spread will be greater. On the basis of this reasoning it is proposed that the ψ_a probability distribution can be represented by the normal probability density function, i.e.,

$$f(\psi_a, \mu_a, \sigma_a) = \frac{e^{-(x-\mu_a)^2/2\sigma_a^2}}{\sigma_a\sqrt{2\pi}}, \quad -\infty < \psi_a < \infty, \quad (12)$$

where μ_a and σ_a are the mean and standard deviation of ψ_a respectively.

[13] In contrast, ψ_b must always be ≥ 0 . In streams where there is a considerable volume of still water, there may be a modal value for the ψ_b probability distribution at $\psi_b = 0$. It is also possible that the distribution of ψ_b will have a second

modal value that is >0 . *Lamouroux et al.* [1995] has noted the existence of bimodal velocity distributions in streams with one of the two modal values at $u = 0$. Given that values of $\psi_b < 0$ are not possible, it is suggested that ψ_b is distributed according to a truncated form of the normal distribution with density function expressed as

$$f(\psi_b, \mu_b, \sigma_b) = \begin{cases} \frac{e^{-(x-\mu_b)^2/2\sigma_b^2}}{\sigma_b\sqrt{2\pi}}, & 0 < \psi_b < \infty \\ 0, & \psi_b < 0. \end{cases} \quad (13)$$

Because this density function truncates the normal distribution at 0, integration of this density function over all possible values will give a value of <1 . To adjust for this, the probability that $\psi_b = 0$ is given by

$$p(\psi_b = 0) = \int_{-\infty}^0 \frac{e^{-(x-\mu_b)^2/2\sigma_b^2}}{\sigma_b\sqrt{2\pi}}. \quad (14)$$

This modification allows for the possibility that the distribution of ψ_b has a modal value at 0 and may have a second mode for some $\psi_b > 0$. To illustrate the effect of truncation, the proposed probability density function for ψ_b is shown in Figure 2 as a frequency histogram for the case of $\mu_b = \sigma_b = 1$.

[14] The method of maximum likelihood [*Devore*, 1987] is used to obtain estimators for the distribution parameters for each of the 149 reach surveys. To calculate the maximum likelihood function used with this method, observed values of ψ_a and ψ_b were each sorted into six categories where these categories are defined so that equal numbers of observations fall into each of the six categories and all observations fall into only one category.

[15] A modified form of the Cauchy distribution was considered but did not conform with the data as well as the normal distribution [*Stewardson*, 1999]. No other simple two-parameter probability density functions were evaluated, because none of the commonly used functions (e.g., log normal, Weibull, and gamma distributions) was consistent with the properties of the ψ_a and ψ_b distributions discussed above. Goodness of fit tests indicate that the normal and truncated normal distributions provide a reasonable fit to the observed distributions of ψ_a and ψ_b , respectively [*Stewardson*, 1999]. Neglecting autocorrelation in the sample data, 70% of the 149 sample data sets are not significantly different (at the 95% level) from the probability density functions given above. This percentage would be larger if autocorrelation in sample data was accounted for in the statistical testing.

[16] To develop a useful stochastic model of the probability distribution of ψ_a and ψ_b , the parameters for the normal and truncated normal distributions (i.e., μ_a , σ_a , μ_b , and σ_b) are related to channel geometry parameters. It is hypothesized that the

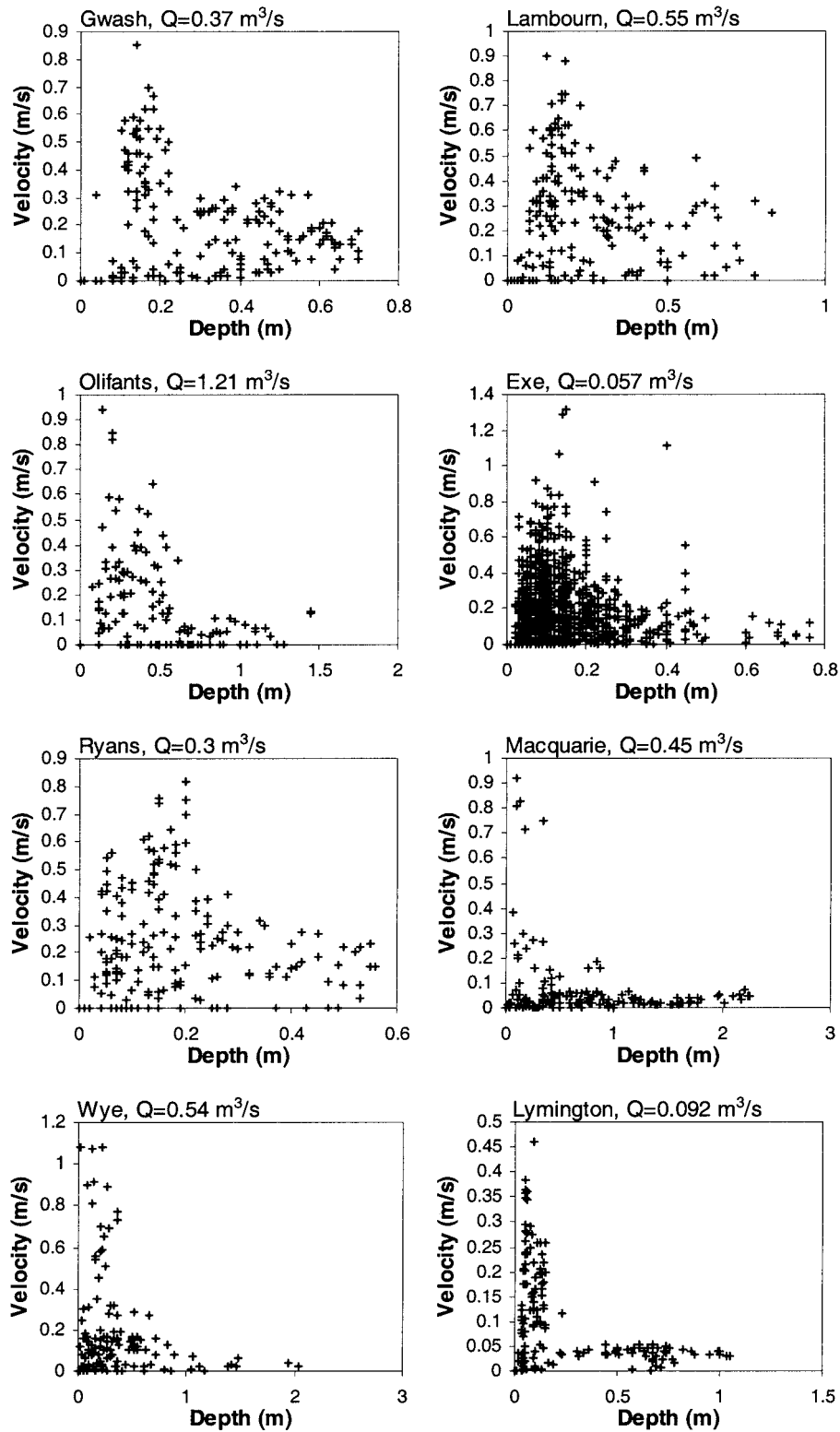


Figure 1. Random samples of velocity and depth in stream reaches.

distribution of ψ_a is related to the distribution of a cross-sectional form of ψ_a defined as

$$\Psi_a = \frac{U}{\sqrt{gD}} - a \ln D, \quad (15)$$

where U is the cross-section velocity ($U = Q/A$) and D is the hydraulic depth ($D = A/W$). It is important to note the distinction between Ψ_a and ψ_a , despite the same form of the equation used for their calculation. The uppercase Greek symbol Ψ_a denotes a cross-sectional hydraulic parameter (calculated using cross-sectional velocity and hydraulic depth), whereas the lowercase

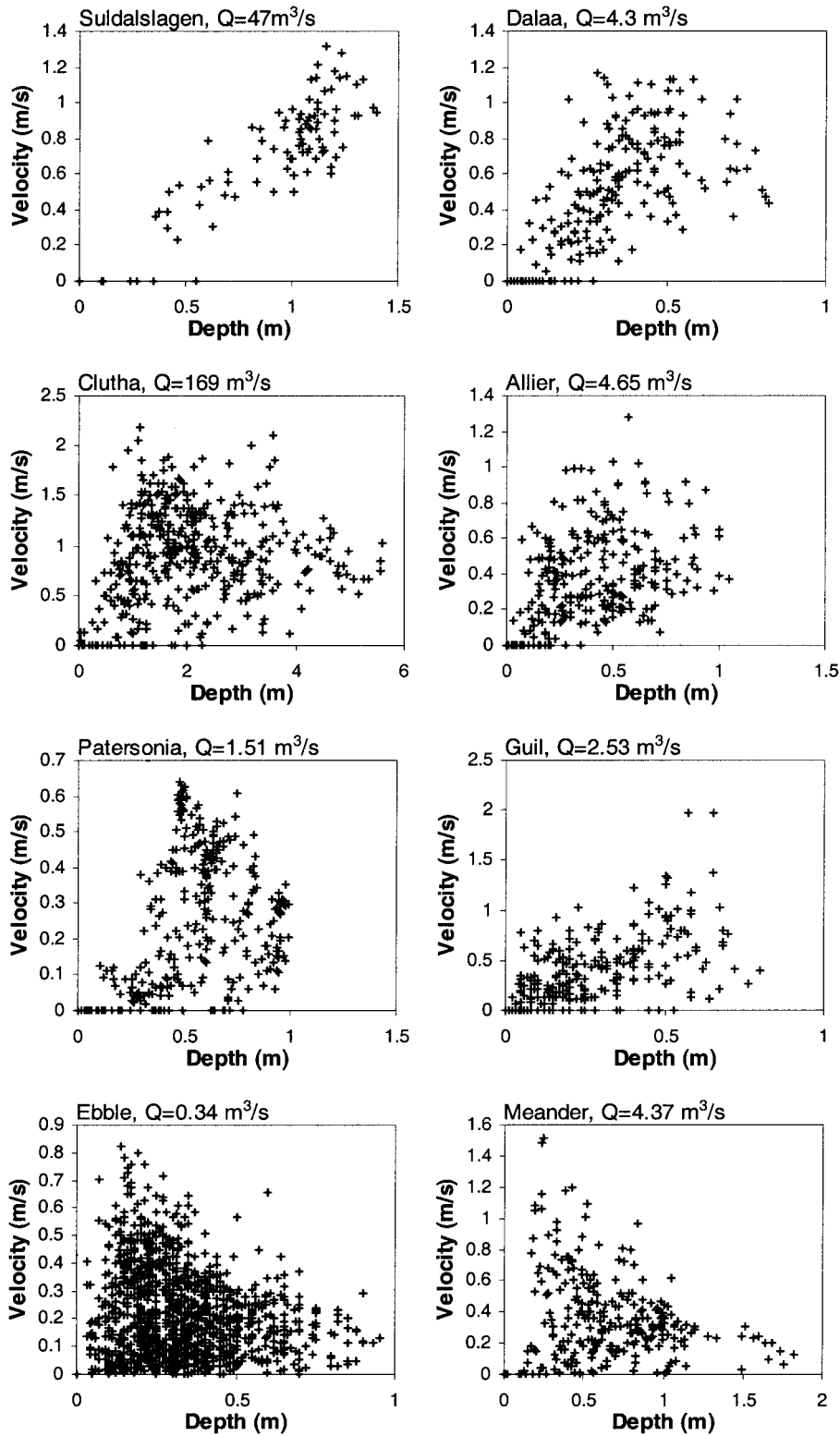


Figure 1. (continued)

symbol ψ_a denotes a variable that may vary across a cross section (calculated using depth-averaged velocity and depth). However, because ψ_a is roughly uniform at a cross section, it might be expected that the mean and standard deviation of ψ_a for a stream reach are closely related to the mean and standard deviation of Ψ_a , respectively.

[17] Since ψ_b is the unit discharge at some point across a cross section, μ_b should be correlated with the mean unit discharge for the reach. The mean unit discharge for a reach can be estimated as Q/\bar{W} , where \bar{W} is the mean water surface width for the reach. It is difficult to anticipate any relation between σ_b and cross-section parameters, as there can be considerable variation in ψ_b within a

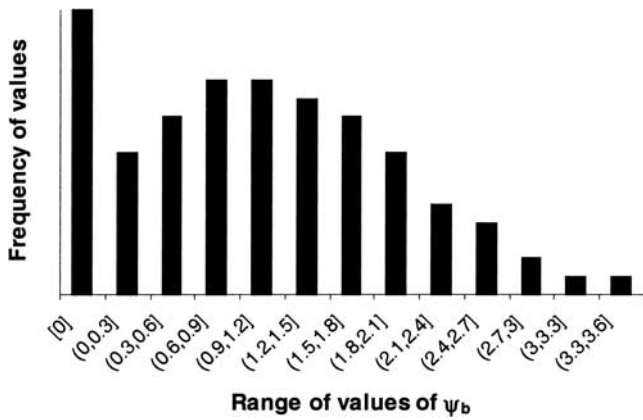


Figure 2. Frequency histogram indicating the proposed probability density function for ψ_b (for this example, $\mu_b = \sigma_b = 1$).

cross section. It might be expected that σ_b is related to μ_b as this parameter has positive values only. However, variability in ψ_b may also be influenced by bed irregularities and flow obstructions that induce irregular flow patterns. Since ψ_b is the product of depth and velocity, it is likely that σ_b is correlated with the standard deviation of depth. Correlation between a range of cross-section parameters and depth variability will be explored using the 149 reach surveys to identify a variable that may predict σ_b .

[18] For the development of the stochastic model, a is treated as a constant for all streams and as invariant with discharge. This simplification is considered acceptable and necessary for the development of the stochastic model using the available data. Further investigations are recommended to elucidate the variables, other than slope, influencing the parameter a and to derive a suitable model for use with the stochastic model described here. Preliminary investigation using the available data failed to provide a model that improved on treating a as a constant. Stewardson [1999] found that using $a = 0.2$ minimized covariance for the 149 reach surveys listed in Table 2, so this value is adopted here for developing the stochastic model. It was also noted that the covariance was relatively insensitive to small adjustments in a , but covariance generally increased as a approached 0. It is argued

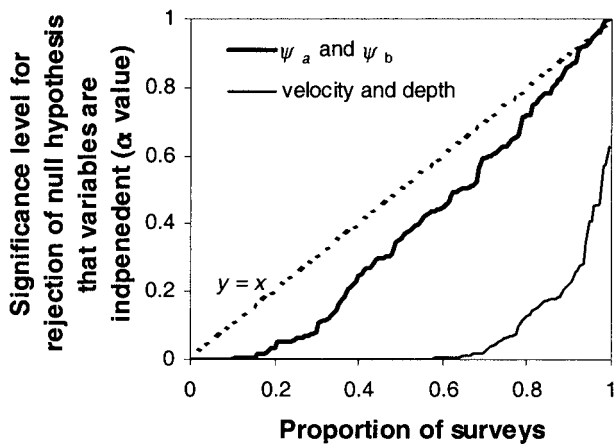


Figure 3. Cumulative distribution of $\phi(\chi^2)$ (a measure of independence of two variables) for 149 χ^2 statistics (if variables are independent, cumulative distribution is expected to coincide with $y = x$).

that the small increase in covariance resulting from treating a as a constant is justified by the increased simplicity of the model.

4. Results

[19] The independence of ψ_a and ψ_b is tested using the χ^2 test of independence and compared with the χ^2 test applied to $baru$ and Z (Figure 3). For this comparison, χ^2 values are transformed to probabilities using the inverse χ^2 function. If the two variables are independent, the resulting probabilities calculated for each of the 149 reach surveys should be uniformly distributed between 0 and 1. The cumulative distribution of the χ^2 probabilities for $baru$ and Z shows a substantially greater number of samples with low probabilities than would be expected if these variables were independent (Figure 3), indicating that $baru$ and Z are generally not independent (i.e., they are related). The null hypothesis of independence of ψ_a and ψ_b would be rejected (with $\alpha = 0.05$) in only 21% of cases, compared to 73% of cases for $baru$ and Z .

[20] Where stream gradient is known, a is calculated using $a = \sqrt{s/\kappa}$ and plotted in Figure 4 against the value of a fitted to minimize the χ^2 statistic (i.e., minimize the covariance of ψ_a and ψ_b). These two estimates of a do not appear to be related, indicating that the calculated value does not provide an estimate of a that minimizes the strength of the relation between ψ_a and ψ_b .

[21] The maximum likelihood estimates of distribution parameters ($\mu_a, \mu_b, \sigma_a,$ and σ_b) show no clear relation between the μ_a and μ_b for the 149 samples (Figure 5a). Most values of μ_a are between 0.1 and 0.8. In contrast, μ_b varies over several orders of magnitude with most values between 0.01 and 1. The variability of ψ_a and ψ_b , expressed as the coefficient of variation (defined as σ/μ), is unrelated (Figure 5b). The standard deviation is generally less than the mean for ψ_a distributions (Figure 5c) but is close to the mean for ψ_b (Figure 5d). The only clear relation between these parameter estimates is a strong positive linear relation between μ_b and σ_b (Figure 5d).

[22] The estimates of μ_a and σ_a are correlated with the mean and standard deviation of Ψ_a , respectively, a cross-sectional form of ψ_a (Figures 6 and 7). Both linear and power law relations were considered for predicting μ_a and σ_a using the mean and standard deviation of Ψ_a , respectively. Power law relations were found to provide better predictions of the probability density function of ψ_a .

[23] The distribution parameter μ_b is correlated with the ratio of discharge to mean water surface width (Figure 8). A power law

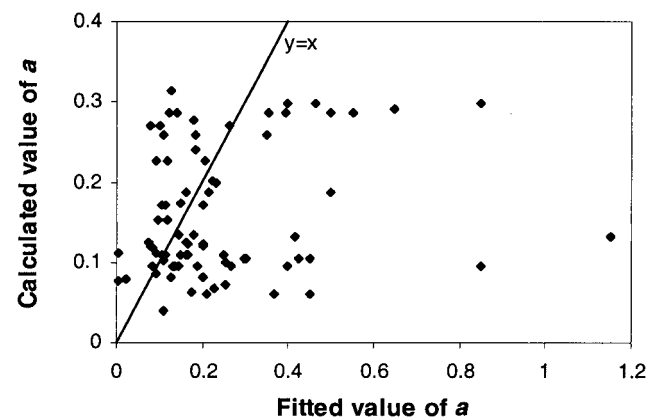


Figure 4. Values of the a parameter estimated using two methods (from theory and by calibration to minimize the covariance of ψ_a and ψ_b).

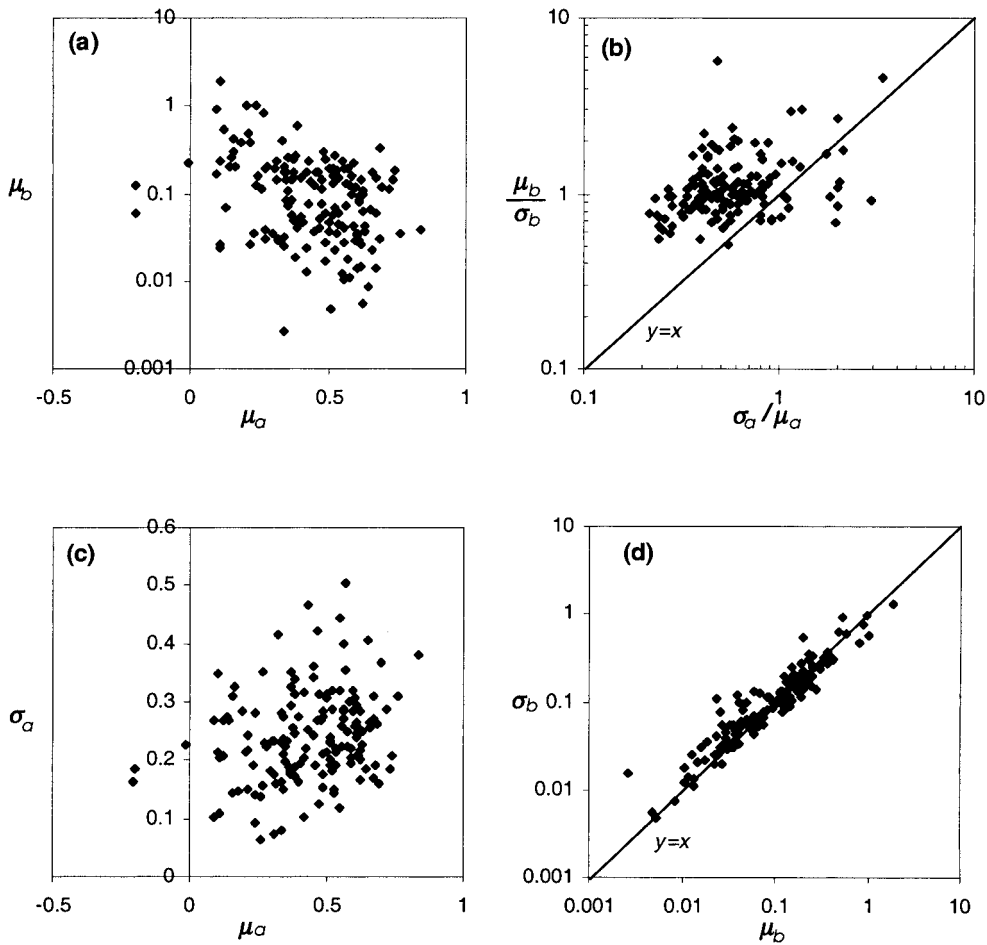


Figure 5. Plots showing parameter estimates for the normal and truncated normal probability density functions of ψ_a and ψ_b , respectively: (a) means of ψ_a and ψ_b , (b) coefficients of variation of ψ_a and ψ_b , (c) mean and standard deviation of ψ_a , and (d) mean and standard deviation of ψ_b .

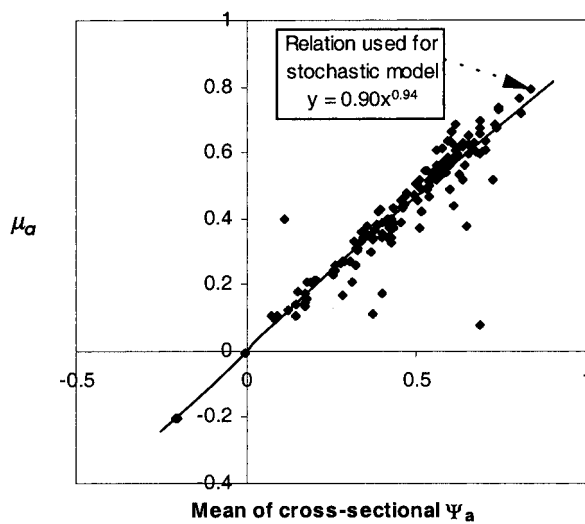


Figure 6. Maximum likelihood estimates of μ_a for the normal approximation of the ψ_a distribution and mean values of Ψ_a (a cross-sectional form of ψ_a) calculated for each of 149 stream surveys.

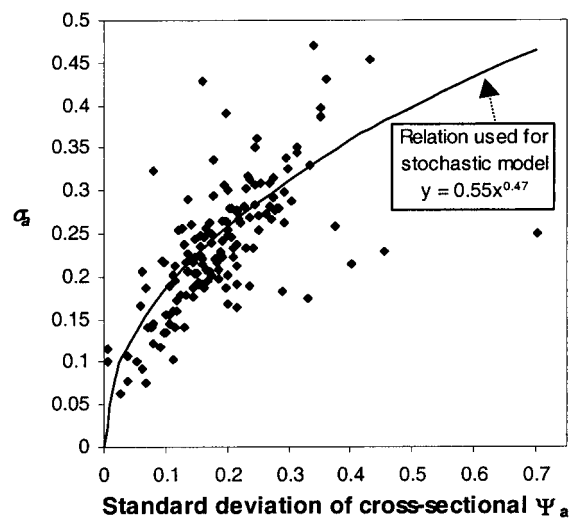


Figure 7. Maximum likelihood estimates of σ_a for the normal approximation of the ψ_a distribution and standard deviation of Ψ_a (a cross-sectional form of ψ_a) for each of 149 stream surveys.

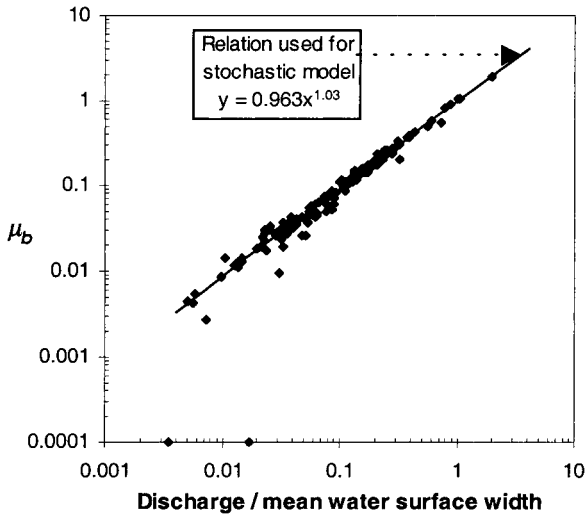


Figure 8. Maximum likelihood estimates of μ_b for the truncated normal distribution and discharge divided by mean water surface width for each of 149 reach surveys.

model best represents this relation. The estimates of σ_b are also correlated with this ratio, although the correlation appears weaker than with μ_b (Figure 9). The correlation between Q/\bar{W} and σ_b reflects the large variation in magnitude of μ_b and the correlation between σ_b and μ_b that is inevitable with distributions of positive values that vary between zero and some upper value. To provide a more reliable estimate of σ_b , factors that may influence the coefficient of variation of ψ_b are examined by plotting them against σ_b/μ_b , a ratio closely related but not equal to the coefficient of variation. Truncation of the normal distribution for ψ_b means that the actual coefficient of variation for the probability density function is less than σ_b/μ_b . Exploration of the data identified two variables that improve the prediction of σ_b : (1) the coefficient of variation of water depth (Figure 10) and (2) the coefficient of variation of water surface width (Figure 11). On the basis of further

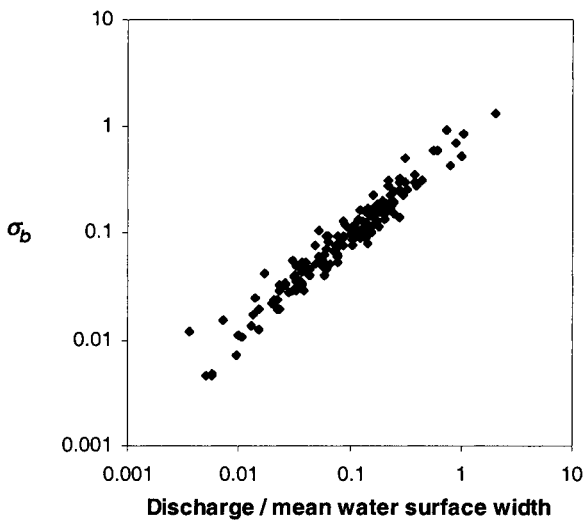


Figure 9. Maximum likelihood estimates of σ_b for the truncated normal approximation of the ψ_b distribution and discharge divided by mean water surface width for each of 149 reach surveys.

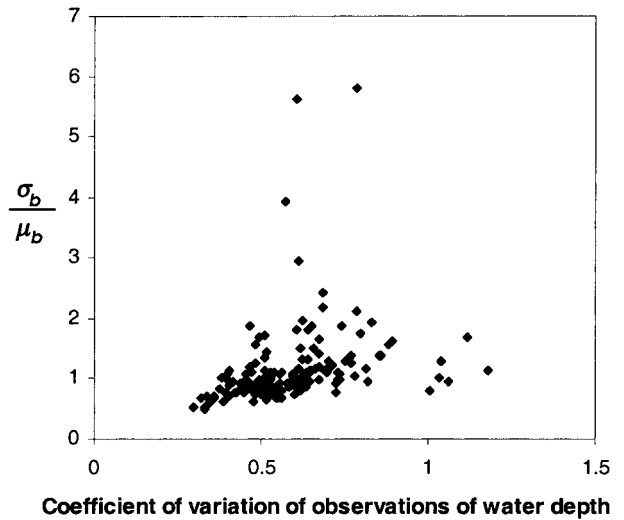


Figure 10. Coefficient of variation of ψ_b calculated using maximum likelihood estimates of μ_a and σ_a for the truncated normal approximation of the ψ_b distribution and the coefficient of variation for measured water depth for each of 149 reach surveys.

inspection of the data the functions proposed for predicting the probability density function parameters are

$$\mu_a = \gamma_1 \bar{\Psi}_a^{\gamma_2}, \tag{16}$$

$$\sigma_a = \gamma_3 (\sigma_{\Psi_a})^{\gamma_4}, \tag{17}$$

$$\mu_b = \gamma_5 (Q/\bar{W})^{\gamma_6}, \tag{18}$$

$$\sigma_b = \gamma_7 (Q/\bar{W})^{\gamma_8} (\sigma_z/\bar{Z})^{\gamma_9} (\sigma_w/\bar{W})^{\gamma_{10}}, \tag{19}$$

where $\gamma_1, \gamma_2, \gamma_3, \dots, \gamma_{10}$ are constants to be set by calibration and σ_z/\bar{Z} and σ_w/\bar{W} are the coefficient of variation of depth and width for the reach, respectively. Values for each of the 10 constants (γ_i ,

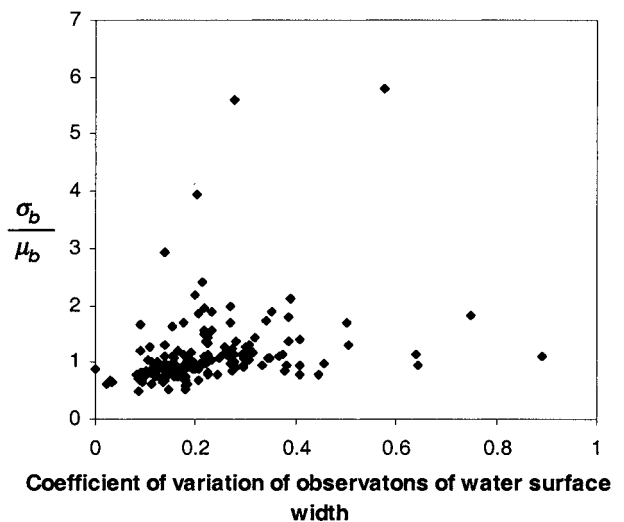


Figure 11. Coefficient of variation of ψ_b calculated maximum likelihood estimates of μ_a and σ_a for the truncated normal approximation of the ψ_b distribution and the coefficient of variation for measured water surface width for each of 149 reach surveys.

Table 3. Calibrated Parameters for the Stochastic Model of ψ_a and ψ_b Probability Density Functions

Parameter	Value
γ_1	0.901
γ_2	0.943
γ_3	0.549
γ_4	0.466
γ_5	0.963
γ_6	1.025
γ_7	1.125
γ_8	0.924
γ_9	0.234
γ_{10}	0.117

where $i = 1-10$) were estimated by calibration to maximize the sum of log likelihood ratios calculated for each of the 149 sites (Table 3).

5. Discussion

[24] This study shows that in contrast to depth-averaged velocity and depth, transformations of these ψ_a and ψ_b do not exhibit a high degree of covariance. Indeed, the relation between ψ_a and ψ_b is sufficiently weak that the assumption of independence is justified for most applications. The residual covariance in the transformed variables could be explained by a number of factors including (1) autocorrelation within samples, (2) spurious

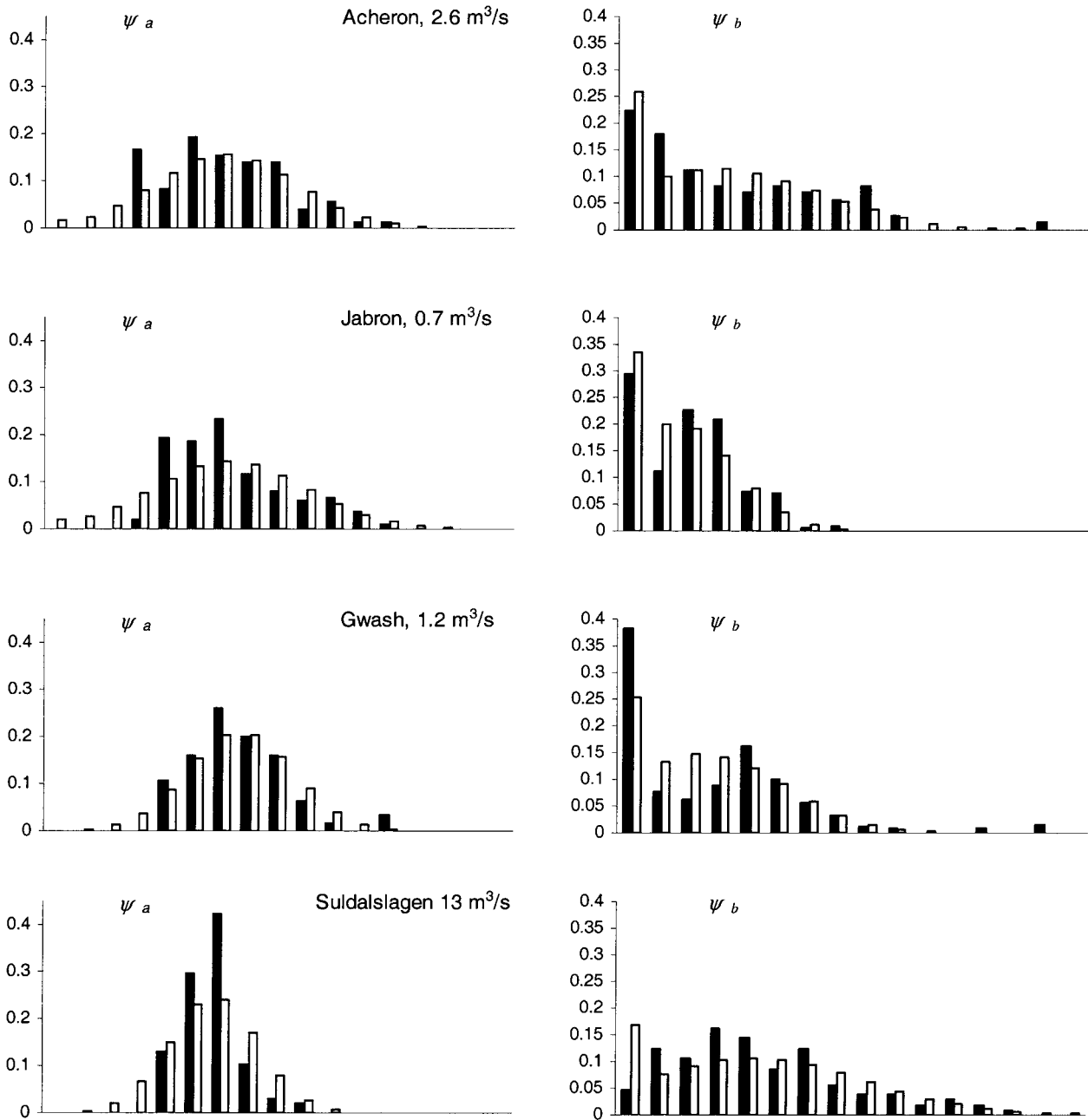


Figure 12. Modeled and observed probability distributions of (left) ψ_a and (right) ψ_b for four sites that show a range of model performance that is representative of the range of model performance for the 149 sites used in this study. Histogram bars represent probabilities for ψ_a in increments of 0.1 starting with $\psi_a \in [-0.2$ to $-0.1)$ and for ψ_b in increments of 0.05 starting with $\psi_b \in [0$ to $0.05)$.

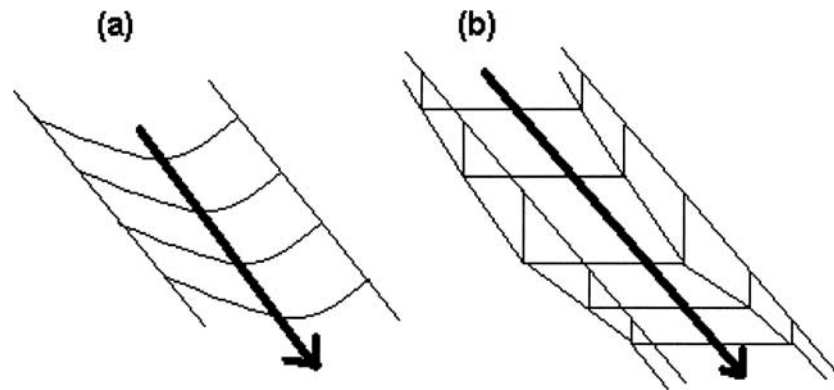


Figure 13. Two idealized channel morphologies: (a) a prismatic channel and (b) a rectangular channel.

correlation, and (3) invalid assumptions in the derivation of the transformations. These factors are discussed in the following paragraphs.

[25] Values of both ψ_a and ψ_b estimated for a cross section will be spatially autocorrelated. A particularly high level of autocorrelation is expected for the variable ψ_a because it is approximately uniform across a cross section. Strictly, the χ^2 test requires that sample values are independent. Autocorrelation in the samples increases the variance in χ^2 statistics for samples of two independent variables. The effect of autocorrelation in these samples could be accounted for in the test by reducing the sample size to an effective sample size [Bayley and Hammersley, 1946] when calculating the test statistics χ^2 . The effective sample size is the equivalent number of independent observations that would provide the same expected variance as the autocorrelated samples, assuming the variables are independent. For ψ_a the effective sample size may be closer to the number of surveyed cross sections than the number of measurement points. Autocorrelation within samples of ψ_a or ψ_b could partly explain the discrepancy between the distribution of the χ^2 statistic for the 149 reach surveys and the expected distribution (see Figure 3).

[26] It is likely that the covariance of ψ_a and ψ_b is in part a result of spurious correlation, because these variables are both calculated using velocity and depth [Benson, 1965]. Random measurement errors in depth and velocity will produce spurious correlation. To remove the effect of spurious correlation, it would be necessary to reduce random errors in the estimation of depth-averaged velocity and depth to insignificant levels. Errors in estimates of depth-averaged velocity are particularly likely if only

a single measurement of velocity is used at each measurement point for most surveys. Failing to account for spurious correlation will bias test results to indicate a stronger relation between the variables than exists in reality.

[27] The derivation of the two transformation (12) and (13) required several assumptions regarding stream hydraulic conditions including a logarithmic velocity profile, a uniform energy gradient and roughness height parameter across each cross section, and a uniform energy gradient along the stream reach. These assumptions may not be valid in some stream reaches. For example, deviations from the logarithmic profile can result from bank drag, large bed roughness (relative to depth), helical motion at meander bends, and the presence of flow obstructions such as large woody debris. Furthermore, energy gradient can vary across the channel if there are body forces acting on the flow such as centrifugal forces at bends and can vary longitudinally as a result of variation in channel geometry. The roughness height parameter may also vary across the channel if there is lateral variation in bed material. It is quite likely that these assumptions are invalid for many streams, particularly at low discharges or where gradients are high. However, the relatively weak relation demonstrated by this study despite the possible violation of simplifying assumptions suggests that the theoretical basis for selecting these two variables is robust.

[28] The results also suggest that the derived expression $a = \sqrt{s/\kappa}$ is not a reliable method for estimating the value of a that minimizes the strength of any relation between ψ_a and ψ_b . A likely explanation for this is that assumptions used in derivation of the transformation are invalid. Consideration of channel irregularities

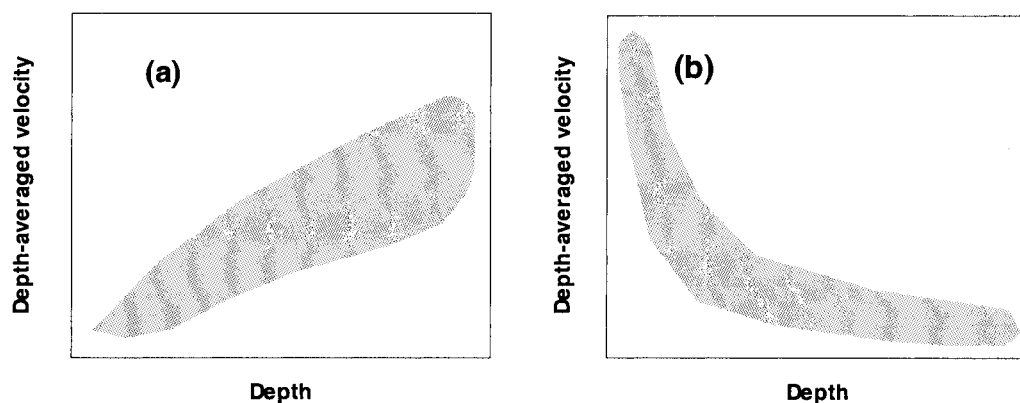


Figure 14. Plots indicating the expected distribution of velocity and depth values in (a) a prismatic channel and (b) a rectangular channel.

that produce flow nonuniformity and secondary currents could provide a more reliable expression for a . Given this result, there is little benefit in using (11) to calculate a for the stochastic model. However, it should be noted that using a fixed value of $a = 0.2$ will slightly increase the covariance of ψ_a and ψ_b .

[29] Aspects of model application including model precision are discussed by Stewardson [1999] and will be the subject of a future publication. A test of the stochastic model using a cross-validation procedure applied to the 149 reach surveys (listed in Table 2) found model error to be within acceptable levels for many applications. Figure 12 shows modeled and observed probability distributions for four sites. Model performance at these four sites is representative of performance at the 149 sites used for model calibration in this study. Stewardson [1999] also compared model errors associated with the stochastic model and a widely used conveyance-type deterministic model. There was no difference in the error of the two models when predicting probability distributions of ψ_a and ψ_b if input data for the two models are estimated directly from reach surveys. However, in many cases, input data are generated using a one-dimensional flow model, and such data are subject to error. The stochastic model was found to be considerably less sensitive to errors in modeled input data than the deterministic model.

[30] Although several substantial simplifying assumptions have been used in the development of the stochastic model, their effect on the usefulness of this approach to quantifying hydraulic variations in stream channels is minimal. The stochastic model relates small-scale two-dimensional hydraulic variations throughout a reach to one-dimensional variations at the scale of channel cross sections. The stochastic model provides an explanation for the different patterns of covariance observed in the depth-velocity samples shown in Figure 1. Some of these plots indicate strong positive correlation between velocity and depth, whereas others show a strong inverse relation. The positive correlation occurs in channels that are more uniform in cross-sectional shape along the channel or at higher flows when longitudinal bed irregularities are less significant. In these channels, variations in ψ_a (along the channel) are considerably less than variations in ψ_b (across the channel). The inverse relation occurs in channels with considerable longitudinal variation in channel morphology and at low flows when these irregularities are more significant. In these channels, variations in ψ_a (along the channel) are greater than variations in ψ_b (across the channel).

[31] The joint probability distribution of velocity and depth varies between two extremes represented by two idealized channels. One extreme case is the prismatic channel with uniform cross-sectional geometry. In this case, there are lateral variations in depth but no longitudinal variation in depth (Figure 13a). A plot of randomly sampled velocity and depth values in the prismatic channel would be expected to look something like that shown in Figure 14a. The second extreme case is a rectangular channel with depth variation in the longitudinal direction associated with undulations in the elevation of the bed but no lateral variation in depth (Figure 13b). Both channels have a uniform width. In this case, velocity and depth would be inversely correlated with lower velocities and higher depths in pool sections. The distribution of velocity and depths in this rectangular channel would resemble the distribution indicated in Figure 14b.

[32] Natural channels tend to vary in both the longitudinal and lateral directions and will have distributions that are somewhere “in between” the two extreme cases shown in Figure 13. Increases in discharge will generally reduce the influence of pool-riffle

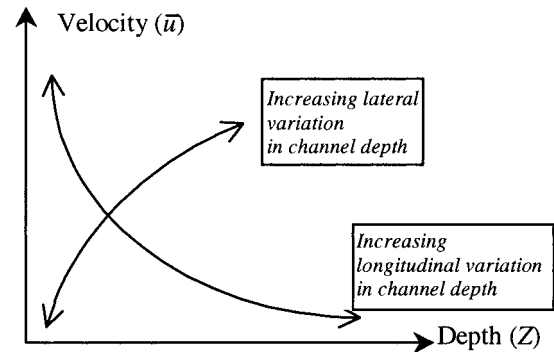


Figure 15. Conceptual diagram indicating how longitudinal and lateral variations in channel depth influence the bivariate probability distribution of \bar{u} and Z .

variations and result in more uniform flow conditions. The variables \bar{u} and Z are distributed with a scatter pattern that is controlled both by longitudinal and lateral depth variations. Lateral variations tend to “stretch” the distribution away from the axes, and longitudinal variations tend to “stretch” the distribution out along the axes (Figure 15). Increasing discharge generally creates more uniform flow conditions and shifts the \bar{u} - Z distribution toward that shown in Figure 13a. To support this explanation of the different patterns of covariance observed in the \bar{u} and Z plots, the distributions shown in Figure 1 are placed in order of increasing longitudinal channel variability. In this case, longitudinal channel variability is measured by the coefficient of variation in cross-sectional area and varies between 0.1 and 1.24. These sample distributions indicate a trend from a positive correlation between \bar{u} and Z (similar to that shown in Figure 14a) to a negative correlation (similar to that shown Figure 14b) with increasing longitudinal channel variability.

[33] The stochastic model provides a simple and reliable approach to modeling hydraulic variations in stream reaches that may be used in a number of ways. The univariate distributions of ψ_a and ψ_b may be converted to a joint distribution of depth and depth-averaged velocity using the Jacobian of the inverse transform (6) and (7). However, the ψ_a and ψ_b distributions are themselves an efficient approach to characterizing hydraulic variations in the stream reaches and should be useful for a range of applications including testing hypotheses regarding the influence of hydraulic variations on stream communities at the reach scale. An advantage of using ψ_a and ψ_b distributions for these studies is that the results can be easily related to channel geometry and discharge using the stochastic model.

6. Conclusion

[34] Spatial variation in velocity and depth is a fundamental characteristic of stream channels. There is strong covariance in these two parameters to be considered if the joint distribution of velocity and depth is to be described. In this paper, depth and velocity are transformed to provide two independent variables ψ_a and ψ_b that vary longitudinally and laterally, respectively, within a stream channel. Although there may be some covariance in these new variables, this is weak compared to covariance of depth and velocity. The assumption of independence is likely to be acceptable for most applications.

[35] The probability distributions of ψ_a and ψ_b can be represented by a normal and a truncated normal density function,

respectively. The truncated function allows for the possibility of a bimodal distribution of ψ_b with a mode at $\psi_b = 0$. The four parameters for these density functions are strongly related to cross-sectional parameters. On the basis of these relations a stochastic model is developed that allows probability distributions of ψ_a and ψ_b to be predicted using cross-sectional geometry data. Input for this model can be easily measured in the field or estimated using a one-dimensional hydraulic model. The stochastic model provides a basis for exploring the relation between channel shape and finer-scale hydraulic variations.

[36] **Acknowledgments.** We gratefully acknowledge the following people and organizations for providing data used in this paper: Nicolas Lamouroux, CEMAGREF, Lyon, France; Mike Dunbar, Ian Johnson, and Craig Elliot, The Institute of Hydrology, United Kingdom; Tim Rhodes, University of Melbourne, Australia; Atle Harby, SINTEF, National Hydraulics Laboratory, Norway; Peter Davies University of Tasmania, Australia; Ian Jowett, National Institute of Water and Atmosphere, New Zealand; and Jackie King, University of Cape Town, South Africa. We also thank Ian O'Neill for his helpful advice on this work. Bruce Rhoads and Robb Jacobson contributed a number of improvements to the clarity of this paper in their reviews of this manuscript.

References

- Allan, J. D., *Stream Ecology. The Structure and Function of Running Waters*, Chapman and Hall, New York, 1995.
- Bayley, G. V., and J. M. Hammersley, The "effective" number of independent observations in an autocorrelated time series, *J. R. Stat. Soc.*, 8, 184–197, 1946.
- Beaumont, G. P., *Intermediate Mathematical Statistics*, Chapman and Hall, New York, 1980.
- Benson, M. A., Spurious correlation in hydraulics and hydrology, *J. Hydraul. Am. Soc. Civ. Eng., Div.*, 91, 35–43, 1965.
- Bovee, K. D., Data collection procedures for the physical habitat simulation system, internal publication, Nat. Biol. Surv., Fort Collins, Colo., 1994.
- Chiu, C., Velocity distribution in open channel flow, *J. Hydraul. Eng.*, 115, 576–594, 1989.
- Devore, J. L., *Probability and Statistics for Engineering and the Sciences*, Brooks/Cole and Nelson, Belmont, Calif., 1987.
- Dingman, S. L., Probability distribution of velocity in natural channel cross sections, *Water Resour. Res.*, 25, 509–518, 1989.
- French, R. H., *Open-Channel Hydraulics*, McGraw-Hill, New York, 1986.
- Lamouroux, N., Depth probability distributions in stream reaches, *J. Hydraul. Eng.*, 124, 224–228, 1998.
- Lamouroux, N., Y. Souchon, and E. Herouin, Predicting velocity frequency distributions in stream reaches, *Water Resour. Res.*, 31, 2367–2375, 1995.
- Leclerc, M., P. Boudreau, J. A. Bechara, and L. Belzile, Numerical method for modelling spawning habitat dynamics of landlocked salmon, *Reg. Rivers Res. Manage.*, 12, 273–285, 1996.
- Milhous, R. T., M. A. Updike, and D. M. Schneider, Physical habitat simulation system reference manual-Version II, in *Instream Flow Information Paper 26, U.S. Fish Wildl. Serv., Div. Biol. Serv. FWS OBS*, 89(16), 1989.
- Singh, K. P., Hydraulic geometry of streams and stream habitat assessment, *J. Water Resour. Plann. Manage.*, 115, 583–597, 1989.
- Stewardson, M. J., Characterising and modelling the hydraulic environment of streams, Ph.D. thesis, Univ. of Melbourne, Melbourne, Victoria, Australia, 1999.

T. A. McMahon and M. J. Stewardson, Department of Civil and Environmental Engineering, Cooperative Research Centre for Catchment Hydrology, University of Melbourne, Parkville, Victoria 3010, Australia. (m.stewardson@civag.unimelb.edu.au)